Temperature dependence of thermoelectric power and thermal conductivity in ferromagnetic shape memory alloy $Ni_{50}Mn_{34}In_{16}$ in magnetic fields

L. S. Sharath Chandra, M. K. Chattopadhyay, V. K. Sharma, and S. B. Roy
Magnetic and Superconducting Materials Section, Raja Ramanna Center for Advanced Technology, Indore, Madhya Pradesh 452 013, India

Sudhir K. Pandey
UGC-DAE Consortium for Scientific Research, Khandwa Road, Indore, Madhya Pradesh 452 001, India
(Received 7 January 2010; revised manuscript received 23 March 2010; published 7 May 2010)

We report a study of the temperature dependence of thermoelectric power S and thermal conductivity κ in the ferromagnetic shape memory alloy $Ni_{50}Mn_{34}In_{16}$ in presence of zero and 20 kOe magnetic field. A peak is observed in both S and κ just below the paramagnetic to ferromagnetic transition temperature (T_C) of this alloy. Further down the temperature another sharp change is observed both in S and κ, and this latter change is associated with the austenite to martensite phase transition in this alloy. The low temperature peak (below $\sim$50 K), which is usually observed in the temperature dependence of S and κ in metallic systems, is absent in the present alloy system. The measured thermal transport properties of $Ni_{50}Mn_{34}In_{16}$ are qualitatively different from those reported earlier for the well known magnetic shape memory alloy system Ni-Mn-Ga. We interpret the measured thermal transport properties using the changes in the electronic structure near the Fermi level. Apart from electronic structure, the scattering of conduction electrons and phonons by the twin boundaries introduced into the system during the martensitic transition also plays an important role in the temperature dependence of S and κ.

DOI: 10.1103/PhysRevB.81.195105 PACS number(s): 72.15.Jf, 72.15.Eb, 75.50.Cc, 81.30.Kf

I. INTRODUCTION

The potential ferromagnetic shape memory (FSM) alloys $Ni_{50}Mn_{50-x}In_x$ (x=14–17) (Refs. 1–7) have been drawing considerable attention for the past few years due to their multi-functional properties such as large magnetocaloric effect (MCE),[5,6] large magnetoresistance (MR), etc.[3] In these alloys the ferromagnetic Curie temperature (T_C) lies just above 300 K, while austenite (AST) to martensite (MST) phase transition takes place in a wide temperature region.[1–3,7] The temperature of this martensitic transition varies from more than 350 K for $x \leq 14$ to less than 200 K for $x \geq 17$. Interestingly, in this range of x, the MST to AST phase transition can be induced by both temperature and magnetic field.[2,3,8] The first order nature of this MST-AST transition is responsible for the above said functional properties.[2,3] Recently, we have shown that the MR, MCE, and the magnetic field induced strain in $Ni_{50}Mn_{34}In_{16}$ alloy are dependent on the therno-magnetic history of the sample.[9–11]

While a considerable amount of experimental results is available in the literature on the magnetic, structural and electrical properties of FSM alloys,[12] there are relatively very few reports on the temperature and magnetic field dependencies of the thermal transport properties.[13–18] Thermal transport data on Ni-Mn-Ga FSM alloys show distinct changes across the T_C and the MST-AST transitions.[14–17] Considerable changes in the thermoelectric power (Seebeck coefficient) are observed in the FSM alloy $Ni_{50}Mn_{36}Sn_{14}$ in presence of magnetic field.[18] In Ni-Mn-In system, Zhang *et al.*, have reported a considerable change in thermal conductivity of $Ni_{50}Mn_{33.7}In_{16.3}$ alloy in presence of magnetic field.[13] These results have motivated us to investigate on the temperature dependence of thermal transport properties of $Ni_{50}Mn_{34}In_{16}$ in presence of applied magnetic fields. In the sections below we present a detailed study of the temperature dependence of thermoelectric power (S) and thermal conductivity (κ) in the presence of zero and 20 kOe applied magnetic field. These results show that (i) both $S(T)$ and $\kappa(T)$ undergo striking change across the paramagnetic to ferromagnetic transition as well as the martensitic transition in $Ni_{50}Mn_{34}In_{16}$; (ii) the overall behavior of $S(T)$ and $\kappa(T)$ are significantly different from that observed earlier for other Heusler alloys and also in ferromagnetic system like Ni.[19–21] We argue that the shape of the 3d spin up and spin down density of states (DOS) and their shifting when temperature is reduced below T_C, and the twin boundaries introduced in the system due to martensitic transition, play very important roles in the thermal transport properties of $Ni_{50}Mn_{34}In_{16}$. Another striking feature revealed in the present study is the absence of the low temperature peak in the temperature dependence of S and κ. We attribute this behavior to the suppression of umklapp phonon-phonon, and phonon-electron process due to scattering from impurities and twin boundaries.

The paper is organized in the following manner. In Sec. II, we present a brief note on sample preparation, the measurement technique and on the method of the electronic structure calculations. In Sec. III, we first describe the results of temperature dependence of thermal transport properties and then introduce the theoretical aspects of $s-d$ scattering and its relevance to Heusler alloys followed by the electronic DOS structure of $Ni_{50}Mn_{34.325}In_{15.625}$ which is closest to the system under experimental investigation. We then present the detailed analysis of the thermal transport properties of $Ni_{50}Mn_{34}In_{16}$ by taking the $s-d$ scattering into consideration. The final conclusions are summarized in Sec. IV.

II. DETAILS OF EXPERIMENTS AND COMPUTATION

The polycrystalline $Ni_{50}Mn_{34}In_{16}$ used in the present experimental study was prepared by arc melting the required amount of constituent pure elements under argon atmosphere. The sample was flipped and remelted several times to ensure homogeneity. The sample was characterized by x-ray diffraction, ac susceptibility, magnetization, and MR etc.[3,5,6,8–11] The S and κ were measured in the temperature range 2.5–320 K for zero and 20 kOe using a Quantum Design Thermal Transport Option (TTO) in a 9T Physical Property Measurement System (PPMS). The sample used for this study was in the form of irregular rod. One end of the sample was connected to the cold head of the TTO puck using a gold coated Cu strip. A heater was attached to the other end of the sample. Two calibrated sensors were used to measure the temperatures of both the ends of the sample. Measurements were carried out in a continuous mode[22] in which a relaxation technique in the frame work given by Maldonado[23] is employed to estimate the S and κ. Here, the temperature of the cold head was continuously varied from an initial value to a final value with a rate of 0.2 K/min or less. A small current pulse was given to the heater. This results in a time varying temperature difference between the two ends of the sample. Temperature of the both the ends were measured and the temperature difference across the sample was calculated over a period of time after switching on and off the heater. Similarly, the thermo emf generated due to the temperature difference across the sample was also measured. The temperature difference and the corresponding emf as function of time were fitted to relaxation equation[22] to estimate the $\kappa(T)$ and S. Since, the sample was not regular, we present only the relative value of $\kappa(T)$ with respect to $\kappa(320\ \mathrm{K})$, so that the errors in the estimation of absolute values of $\kappa(T)$ are avoided.

The electronic structure calculations for $Ni_{50}Mn_{34.325}In_{15.625}$ in both the paramagnetic and ferromagnetic state were carried out using state-of-the-art full potential linearized augmented plane-wave (FP-LAPW) method.[24] The lattice parameter of 6.011 Å and $L2_1$ structure[9] were used for the calculations. The Muffin-Tin sphere radii were chosen to be 2.322, 2.281, and 2.549 a.u. for Ni, Mn, and In atoms, respectively. For the exchange-correlation functional, we have adopted recently developed generalized gradient approximation (GGA) form of Perdew *et al.*[25] The self-consistency was achieved by demanding the root mean square (RMS) change in the effective potential and magnetic field to be smaller than 10^{-4}. The density of states were calculated using 200 k-point mesh in the Brillouin zone.

The composition $Ni_{50}Mn_{34.325}In_{15.625}$ is chosen due to the calculation of DOS for $Ni_{50}Mn_{34}In_{16}$ is almost impossible for us as it cost huge computational time. The $Ni_{50}Mn_{34.325}In_{15.625}$ is the nearest composition for which electronic structure calculation is possible through 32 atom super cell configuration and for this composition, the sample undergoes martensitic transition below in the ferromagnetic state.[1]

III. RESULTS AND DISCUSSION

Figure 1 shows the temperature dependence of S in $Ni_{50}Mn_{34}In_{16}$ for magnetic field $H=0$ and $H=20$ kOe. $S(T)$ is negative in the entire temperature range of interest. In the paramagnetic state, S is about $-10.5\ \mu\mathrm{V/K}$ at 315 K. As temperature is decreased, S increases in the negative direction. A change of slope in $S(T)$ occurs around 302 K, and this temperature roughly coincides with T_C of $Ni_{50}Mn_{34}In_{16}$.[3] Similar change in slope around T_C has earlier been observed for Ni (Refs. 19 and 20) and Ni-Mn-Ga.[15] However, $S(T)$ decreases sharply in magnitude below 298 K giving rise to a negative peak in $S(T)$. Such a behavior of $S(T)$ across T_C is different from what has been observed for Ni and Ni-Mn-Ga. $S(T)$ measured across the T_C in the presence of an applied magnetic field, does not show any significant change in the behavior. When temperature is further decreased below 290 K, there is a sharp drop in the magnitude of $S(T)$ at about 240 K. We attribute this sharp change to the AST-MST transition in $Ni_{50}Mn_{34}In_{16}$.[3] Across this transition, hysteresis between warming and cooling cycle is observed over a wide range of temperature. This hysteresis is related to the disorder influenced first order nature of this AST-MST phase transition[26] and agrees well with the other measurements.[3,6,9,11] With an applied field of 20 kOe, the drop in $S(T)$ occurs at 230 K. This is because of the shift in the AST-MST transition to lower temperatures with an applied magnetic field. Well below the AST-MST transition there is again no significant field dependence of $S(T)$. It is also interesting to note that, $S(T)$ is linear below this transition without any signature of phonon drag effect.[19]

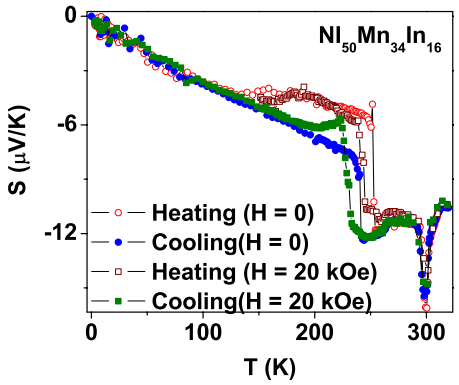

FIG. 1. (Color online) Thermopower of $Ni_{50}Mn_{34}In_{16}$ in the temperature range 2.5 to 320 K in presence of zero and 20 kOe magnetic field. The Curie temperature is characterized by a slope change at 302 K. A large negative peak just below T_c is observed (see text for details). A sharp jump is seen across MST-AST transition. This transition shifts to lower temperature in presence of magnetic field. At low temperatures, the characteristic peak in S corresponding to phonon drag effect is absent here.

Figure 2 shows the $\kappa/\kappa_{320\ \mathrm{K}}$ verses T plot for $Ni_{50}Mn_{34}In_{16}$. A sharp peak in $\kappa(T)$ is observed in the temperature regime, which coincides with the paramagnetic to ferromagnetic transition. This behavior is in sharp contrast with what has been observed in a sample with nearby concentration $Ni_{50}Mn_{33.7}In_{16.3}$,[13] as well as Ni-Mn-Ga.[15] Normally, a change of slope in $\kappa(T)$ is observed across the Curie temperature for the transition metal ferromagnets.[21] On decreasing the temperature further below T_C, $\kappa(T)$ suddenly drops across the AST-MST transition around 240 K. A marked hysteresis in $\kappa(T)$ is observed between heating and

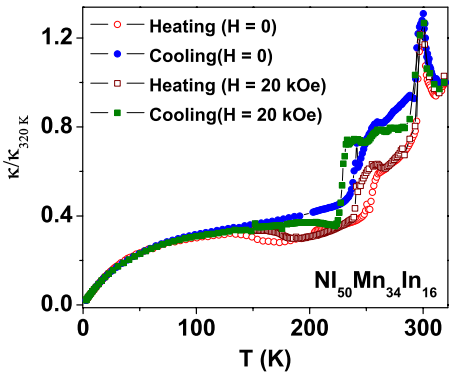

FIG. 2. (Color online) Thermal Conductivity of $Ni_{50}Mn_{34}In_{16}$ in the temperature range 2.5 to 320 K in presence of zero and 20 kOe magnetic field. The T_c is characterized by a jump at 303 K. A sharp drop due to martensitic transition is observed at 240 K when temperature is reduced.

cooling cycle across this AST-MST transition. Application of a magnetic field of 20 kOe also has a significant effect on $\kappa(T)$ in the temperature region around the AST-MST transition.

A peak in $\kappa(T)$ is generally expected at low temperatures for metallic samples due to the phonon umklapp process.[27] This characteristic peak in $\kappa(T)$ is absent in the present sample, and $\kappa(T)$ decreases rather monotonically in the MST phase of $Ni_{50}Mn_{34}In_{16}$.

The magnetism, and electrical transport properties of Heusler alloys can be understood using the $s-d$ interaction.[28–31] Using the same interaction mechanism the properties of Ni across the T_C were also explained.[19,20] In the paramagnetic state of Ni-Mn based Heusler alloys, Ni $3d$ band is nearly full, where as, the Mn $3d$ band is half filled.[32] As the temperature is decreased below T_C, the Mn $3d$ spin up (spin down) band is shifted below (above) the E_F. This results in draining out (filling up) of spin down (up) band.[32] Hence, there is a temperature dependent behavior of $s-d$ scattering. As a consequence, drastic changes can be observed in the temperature dependence of transport properties. This aspect is discussed below to explain the thermal transport properties of $Ni_{50}Mn_{34}In_{16}$.

A. Contributions from $s-d$ scattering to the transport properties

In case of $s-d$ scattering, the energy dependent electrical conductivity can be expressed as[19]

$$\sigma(E_F) = e^2 K_{n=0} = \frac{2}{3} e^2 u^2 \frac{N_s(E_F)}{N_d(E_F)}, \tag{1}$$

where e is the electronic charge, u is the drift velocity. The $N_s(E_F)$ and $N_d(E_F)$ are the DOS of conduction and d electrons at E_F, respectively. The K_n is the transport integral and is given by[27]

$$K_n = \frac{1}{e^2} \int_{\infty}^{-\infty} (\omega - E_F)^n \left(-\frac{\partial f}{\partial \omega} \right) \sigma(\omega) d\omega, \tag{2}$$

where f is the Fermi function. Then S and electronic part of thermal conductivity κ_e can be expressed as[20]

$$S = -\frac{1}{eT} \frac{K_1}{K_0} \tag{3}$$

and

$$\kappa_e = \frac{1}{T} \left(K_2 - \frac{K_1^2}{K_0} \right). \tag{4}$$

The temperature dependence of transport properties for $k_B T \ll E_F$ (k_B is the Boltzmann constant) can be extracted using Sommerfeld expansion of K_n. Then for a ferromagnetic state, σ, S, and K can be expressed as[20]

$$\sigma(E_F) = \frac{2}{3} e^2 u^2 \frac{N_s(E_F)}{N_{d\uparrow}(E_F) + N_{d\downarrow}(E_F)}, \tag{5}$$

$$S = -\frac{\pi^2 k_B^2 T}{3e} \left[\frac{1}{N_s} \frac{\partial N_s(\omega)}{\partial \omega} - \frac{\left(\frac{\partial N_{d\uparrow}(\omega)}{\partial \omega} + \frac{\partial N_{d\downarrow}(\omega)}{\partial \omega} \right)}{N_{d\uparrow} + N_{d\downarrow}} \right]_{\omega = E_F} \tag{6}$$

and

$$\kappa_e = L_0 T \frac{2}{3} e^2 u^2 \frac{N_s(\omega)}{N_{d\uparrow}(\omega) + N_{d\downarrow}(\omega)}, \tag{7}$$

where $N_{d\uparrow}$ and $N_{d\downarrow}$ are the up spin and down spin d-DOS, respectively. Here the transport properties are governed by the changes in the d-DOS. In case of ferromagnets, spin up and spin down DOS will split and move against each other when the temperature is decreased below T_C. The loss of d-DOS at E_F and the changes in $\frac{\partial N_{d\uparrow}(\omega)}{\partial \omega}$ and $\frac{\partial N_{d\downarrow}(\omega)}{\partial \omega}$ at E_F due to the shifting in bands explain to a first approximation, the behavior of σ, S, and κ across the T_c in Nickel.[21]

B. Electronic structure of $Ni_{50}Mn_{34}In_{16}$

The partial DOS structures of Ni, Mn, and In for $Ni_{50}Mn_{34.325}In_{15.625}$ are shown in Fig. 3 for both nonmagnetic (paramagnetic) and ferromagnetic cases. In the paramagnetic state, the Mn and Ni $3d$ DOS are dominant near the Fermi level. The In $5p$ and $5s$ states are very small in the paramagnetic state and remains nearly same in ferromagnetic state also. As the temperature is reduced below T_C, the Mn $3d$ states will split into up spin and down spin bands and move downwards and upwards with respect to the Fermi level, respectively. We also find there are considerable changes in the Ni $3d$ DOS structure.

C. Thermoelectric power

The thermoelectric power of $Ni_{50}Mn_{34}In_{16}$ can be understood if we apply the Eq. (6). to the calculated DOS structure at the Fermi level. The major contribution to S is arising

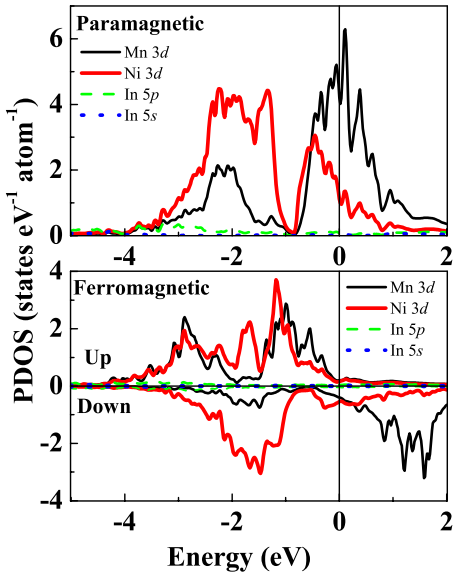

FIG. 3. (Color online) Density of states for $Ni_{50}Mn_{34.325}In_{15.625}$, which is closest to the present system under experimental investigation. In the paramagnetic state, Mn 3*d* and Ni 3*d* partial DOS (PDOS) are dominant at E_F. The Mn 3*d* and Ni 3*d* PDOS at E_F are reduced in the ferromagnetic state. The In 5*p* and 5*s* states are small in the paramagnetic state and in ferromagnetic state, these states mostly remains same as in the paramagnetic state.

from the N_s which consists of In 5*p* and 5*s* states. At E_F, N_s is broad and very small (Fig. 3). As $S \approx (\frac{1}{N_s}\frac{\partial N_s}{\partial \omega})_{\omega=E_F}$ [first term in the Eq. (6)], we find large negative S at high temperatures. This is true for most of the Heusler alloys.[15,18,33] The second term in the Eq. (6). can account for the changes in the $S(T)$ across the T_C (Fig. 4). The changes in N_d and $(\frac{\partial N_d}{\partial \omega})_{\omega=E_F}$ when temperature is decreased below T_C are summarized below.

(a) The $N_{d\uparrow}(E_F)$ of Mn 3*d* decreases and its derivative $\frac{\partial N_{d\uparrow}(\omega)}{\partial \omega}$ at E_F varies from negative value at near T_C to zero at far below T_C.

(b) The $N_{d\downarrow}(E_F)$ of Mn 3*d* decreases and its derivative $\frac{\partial N_{d\downarrow}(\omega)}{\partial \omega}$ at E_F varies from positive value at near T_C to lower positive value at far below T_C.

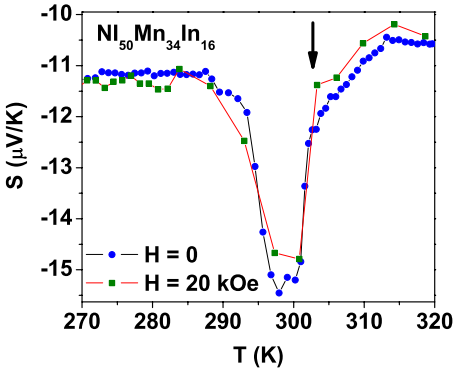

FIG. 4. (Color online) Thermopower near the Curie temperature of $Ni_{50}Mn_{34}In_{16}$ in presence of zero and 20 kOe magnetic field for the cooling cycle.

(c) The both $N_{d\uparrow}(E_F)$ and $N_{d\downarrow}(E_F)$ of Ni 3*d* decreases and their derivatives $\frac{\partial N_{d\uparrow}(\omega)}{\partial \omega}$ and $\frac{\partial N_{d\downarrow}(\omega)}{\partial \omega}$ at E_F vary from negative value at near T_C to zero at far below T_C.

Hence, near T_C, the absolute value of S increases as all the DOS except Mn 3*d* spin down band are contributing a negative thermoelectric power. However, when temperature is further lowered, the contributions from Ni 3*d* and Mn 3*d* spin band vanish as derivatives of these DOS structures approaches to zero and the only contributing term is from Mn spin down band which is positive. Hence, we observe a decrease in absolute S. In other words, the changes in the electronic DOS structure below the ferromagnetic state are responsible for the changes in the thermoelectric power.

When temperature is further decreased in zero magnetic field, a sharp jump of about ~5 μV/K is observed at the martensitic transition at about 240 K having a width of 1 K. It is observed that the jump in S across the first order structural transition is common in many of the systems such as NiTi,[34] Ce_3Al,[35] Gd_5Ge_4, and related alloys,[36–39] and $Ni_{50-x}Mn_{25+x}Ga_{25}$,[15] etc. It is also observed that the width of the jump is over several Kelvin for the case of non magnetic systems like NiTi and Ce_3Al etc. and is very sharp when such a transition is coupled with a magnetic transition like in the systems Gd_5Ge_4 or structural transition in the ferromagnetic state like $Ni_{50-x}Mn_{25+x}Ga_{25}$, $Tb_5(Si_{0.5}Ge_{0.5})_4$ (Ref. 38), etc. In the present case, the AST-MST transition is also associated with a marked drop in magnetization.[6] And, we notice that similar to the cases of $Ni_{50-x}Mn_{25+x}Ga_{25}$, $Tb_5(Si_{0.5}Ge_{0.5})_4$ and Gd_5Ge_4 the jump in $S(T)$ is also quite sharp across the AST-MST structural transition in $Ni_{50}Mn_{34}In_{16}$. For the cooling cycle, the jump in the absolute thermopower across the structural transition can be from a lower value to a higher value,[15,34] or from a higher value to a lower value.[35–40] This can be understood by considering the changes in the electronic structure at the Fermi level across the martensitic transition. It is to be noted here that the overall electronic structure do not change much across the martensitic transition, but the Fermi level shifts either upwards or down wards. Below the structural transition, there is a loss of DOS at E_F for NiTi (Ref. 41) and Ni-Mn-Ga.[42,43] Hence, for the cooling cycle, the observed jump in $S(T)$ is from a lower value to a higher value. In case of Fe_2VAl, there is an enhancement of DOS at E_F below the structural transition.[40] Here, during cooling, the observed jump in $S(T)$ is from a higher value to a lower value. Hence, the drop in S across the MST transition for the present sample can be inferred to be due to an enhancement of DOS at E_F. The shift in the Fermi level can be estimated by considering a linear temperature dependence of $S = \pi^2 k_B^2 T / 2eE_F$ at low temperatures.[19] The $S(T)$ is linear below martensitic transition. The slope of the linear fit (solid red line in Fig. 5) to $S(T)$ in MST phase can be used to estimate E_F for the MST phase and is about 1.2 eV. In order to estimate the E_F for the AST phase, a hypothetical linear temperature dependence of $S(T)$ at low temperatures for the AST phase can be assumed as that shown by a solid black line in the Fig. 5. It is supported by our 20 kOe data where a quasi linear temperature dependence of S is observed between MST start temperature of $H=20$ kOe and $H=0$. The E_F estimated from this, is about 0.74 eV. Hence, the shift in the Fermi level across the maartensitic

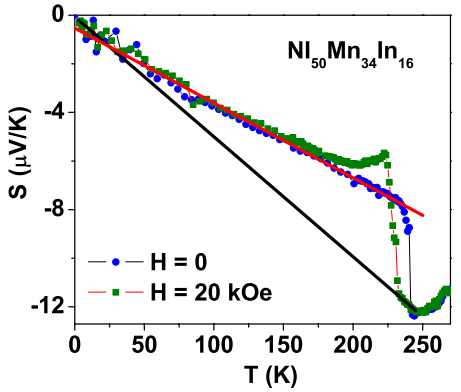

FIG. 5. (Color online) Temperature dependence of S for cooling in presence of zero and 20 kOe magnetic field. The solid black line is the hypothetical line representing temperature dependence of S in the AST phase at low temperature. The solid red line is the linear fit to experimental data points below martensitic transition.

transition is about 0.46 eV. This is in agreement with the theoretical calculations for Ni-Mn-Ga systems.[42,43]

In metals, normally a peak in $S(T)$ is observed below 50 K. This is associated with the phonon-electron umklapp scattering. Here, the electrons gain momentum when they are scattered by low energy phonons, leading to a positive peak in $S(T)$.[19] This is called phonon drag thermopower and is observed for Ni-Mn-Ga alloys also. However, there is no such peak in $Ni_{50}Mn_{34}In_{16}$. The $S(T)$ is extremely linear in the temperature range 2.5 to 230 K. In the MST phase, twin boundaries and the impurities due to surface relief can contribute to the scattering of phonons and electrons. If the size of the twin boundaries is of the order of wavelength of the phonons present at that temperature, then the phonons are normally scattered by these twin boundaries. Apart from this, relaxation time corresponding to phonon-impurity scattering is also high. When such scattering is present, less phonon momentum is imparted to the conduction electrons and the corresponding peak in $S(T)$ reduces or disappears.[19] Similarly, scattering of electrons from the twin boundaries and the impurities in the MST phase suppresses the electron-phonon umklapp scattering. This also contributes to the suppression of the phonon drag thermoelectric power.

D. Thermal conductivity

Normally, there is a change in slope in σ, S, and κ at the T_c. This can be explained by Eqs. (5)–(7). However, temperature dependence of transport properties of transition metals cannot be explained by these equations.[45] It is also true for changes in κ around T_c for $Ni_{50}Mn_{25}Ga_{25}$,[15] and Gd (Ref. 46) as well as in our present data on $Ni_{50}Mn_{34}In_{16}$ (Fig. 6). This discrepancy is due to the omission of higher order terms in deriving Eq. (7). Temperature dependence of S shows that there is considerable contribution from derivatives of the DOS at E_F. Hence, in order to explain the changes in κ near the T_c one needs to consider higher order terms. The higher order correction to κ_e is given by

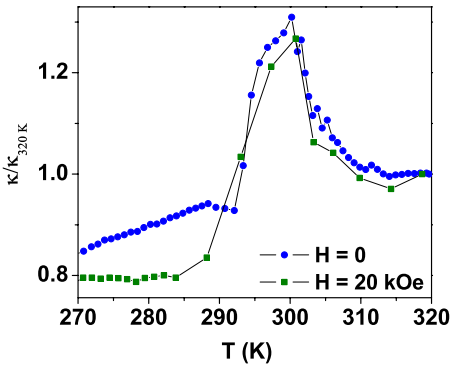

FIG. 6. (Color online) Temperature dependence of κ near T_c for the cooling cycle. Higher order corrections for κ_e is required to explain the changes around T_c.

$$\Delta\kappa_e \propto T^3\left[0.46\frac{N_s(\omega)}{N_d^3(\omega)}\left(\frac{\partial N_d(\omega)}{\partial\omega}\right)^2 - 0.35\frac{N_s(\omega)}{N_d^2(\omega)}\frac{\partial^2 N_d(\omega)}{\partial\omega^2} + \ldots.\right]. \quad (8)$$

This correction needs to be incorporated in to Eq. (7), after taking the spin splitting into consideration. This is because, $\Delta\kappa_e$ will be very large and can have either sign depending upon the contributions from higher order derivatives. These contributions can become large when a large DOS is present in a narrow energy range and/or deviation from parabolic nature of DOS fails to exist.

Apart from the variations around T_C, κ is temperature dependent below T_C. Generally, for a normal metal, $\sigma \propto T^{-1}$ at high temperatures, leading to a constant κ_e. However, in case of $s-d$ scattering σ is not proportional to T^{-1}. Hence, we find temperature dependence of κ_e.

There is a sharp drop in κ across the martensitic transition when temperature is decreased below 250 K. Note that the results of $S(T)$ studies discussed above suggest that there is an increase in the DOS at the Fermi level. Hence, one expects an increase in σ and κ below the martensitic transition. However, this is in contradiction with the observed results of σ and κ. This is because of the dominance of scattering of phonons and electrons from the impurities and twin boundaries which suppresses the effects due to an enhancement of the DOS at E_F. Hence, both electrical and thermal conductivities decrease at the AST to martensitic transition.

In general thermal conductivity can be expressed as $\kappa = \kappa_e + \kappa_L$, where κ_L is the lattice thermal conductivity and is given by $\kappa_L = \frac{1}{3}C_v v^2 \tau$, where C_v is the lattice heat capacity, v is the group velocity of phonons, and τ is the relaxation time. At high temperatures, phonon-phonon interactions dominate and the corresponding τ is inversely proportional to temperature.[19,44] Phonon heat capacity at these temperatures is independent of temperature and hence, $\kappa_L \propto T^{-1}$. Here, for metals, κ is dominated by κ_e. In the low temperature limit, only long wavelength phonons exist and hence impurity-phonon and phonon-boundary scattering dominates leading to temperature independent τ.[19,44] At these temperatures, lattice heat capacity varies as T^3 leading to $\kappa_L \propto T^3$. In addition, κ_e will be linear in T. At intermediate temperatures, umklapp

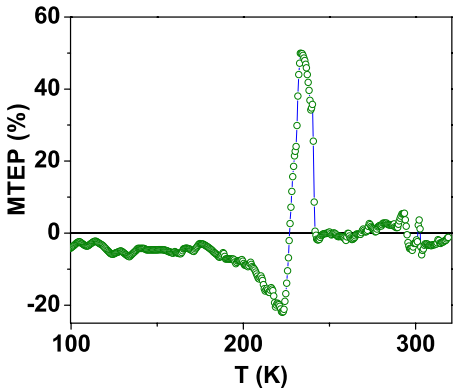

FIG. 7. (Color online) Temperature dependence of magnetothermoelectric power (MTEP) for $H=20$ kOe for the cooling cycle in $Ni_{50}Mn_{34}In_{16}$. MTEP is very large across the AST-MST phase transition and is almost zero otherwise.

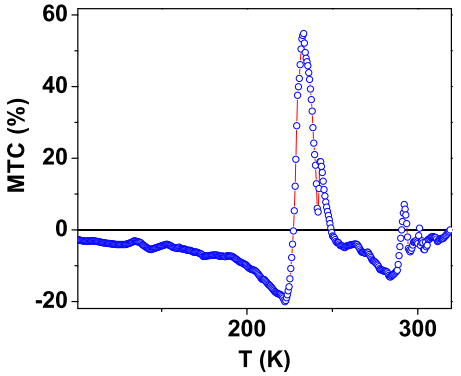

FIG. 8. (Color online) Temperature dependence of magnetothermal conductivity (MTC) for $H=20$ kOe for the cooling cycle in $Ni_{50}Mn_{34}In_{16}$. MTC is very large across the AST-MST phase transition and is also significant in the AST phase below T_c.

phonon-phonon interaction dominates leading to $\tau \propto \exp(\Theta_d/T)$.[19,44] Here, lattice heat capacity is slow varying function of temperature leading to $\kappa_L \propto \exp(\Theta_d/T)$. Hence, for a metal, a peak in the temperature dependence of thermal conductivity occurs at low temperatures.

However, when impurity level is fairly large, effect due to phonon-impurity scattering can be seen even at high temperature. As said earlier, this scattering also leads to suppression of umklapp scattering. Hence, temperature dependence of κ_L is seen as T^3 at low temperatures and constant at high temperatures. Similarly, at low temperatures, the scattering of electrons from impurities leads to $\kappa_e \propto T$ as σ become independent of temperature. Hence, in our data, the peak in κ at low temperatures is absent (Fig. 2). This is supported by the large residual resistivity of 250 $\mu\Omega$ cm in the MST phase.[3]

E. Effect of magnetic field on the thermal transport properties of $Ni_{50}Mn_{34}In_{16}$

The MST to AST phase transition in $Ni_{50}Mn_{34}In_{16}$ can be driven either by temperature or by magnetic field.[3] The drop in $S(T)$ at AST-MST phase transition at 240 K shifts to 230 K in presence of 20 kOe of magnetic field. This is because of the shift in the AST-MST transition to lower temperatures with an applied magnetic field.[3] Hence, there is a large magnetothermoelectric power (MTEP$=[S_H-S_{H=0}]\times 100/S_{H=0}$) across the AST-MST phase transition. Figure 7 shows the temperature dependence of MTEP for $H=20$ kOe. MTEP is about 50% around the martensitic transition and is almost zero otherwise. This magnitude is similar to that of MR observed across the AST-MST transition in $Ni_{50}Mn_{34}In_{16}$.[3] From Eq. (3). it can be shown that the MTEP is proportional to $[(\rho_H(\frac{d\rho_0/\rho_H}{dw})-\rho_0)/\rho_0]_{w=E_F}$. Since, $(\rho_0/\rho_H)_{w=E_F}>1$, we expect MTEP should be proportional to MR. The MR is negative in this system.[3] This means that the MTEP should be negative. However, we have observed a positive MTEP. This indicates the mechanisms that are governing the MTEP and MR are different. As said earlier, the changes in the MTEP is mainly due to shift in the Fermi level resulting in the drop in the absolute value of S. However, scattering of electrons by the twin boundaries do not effect S much at these temperatures. But, in case of resistivity, formation of twin boundaries and the surface reliefs contribute heavily as compared to the changes in the Fermi surface. Hence, we observe a positive MTEP where MR is negative. There is a change of sign in MTEP below the AST to MST transition. We do not have any straightforward explanation for this behavior right now.

An application of magnetic field of 20 kOe also has a significant effect on $\kappa(T)$ in the temperature region around the AST-MST transition. Figure 8 shows the temperature dependence of magnetothermal conductivity (MTC $=[\kappa_H-\kappa_{H=0}]\times 100/\kappa_{H=0}$) for $H=20$ kOe. Similar to MTEP, MTC is large across the AST-MST transition and the magnitude is similar to MTEP and MR. In contrast to MTEP, MTC is also significant in the AST phase below T_C. The change of sign in MTC below the AST-MST transition is similar to MTEP. In Ni-Mn-In systems, Zhang *et al.* have shown that the Wiedemann-Franz law is valid below T_C.[13] In such cases, the κ_e can be expressed as $L_0T\sigma$ [from Eq. (4)]. Hence, MTC is proportional to -MR. Since, MR is negative in these systems we found a positive MTC which is in agreement with the observations of Zhang *et al.*[13] Hence, it appears that the electrical and thermal conductivities across the MST-AST phase transition are governed by twin boundary scattering while thermoelectric power across the MST-AST phase transition is governed by changes in the electronic structure. These lead to correlation between MTC and MR while MTEP shows no correlation with the MR.

IV. CONCLUSION

In conclusion, we have measured the thermoelectric power and thermal conductivity of $Ni_{50}Mn_{34}In_{16}$ in presence of zero and 20 kOe magnetic field. An anomalous peak just below T_c in the temperature dependence of S and κ is shown to be due to the shape of the $3d$ spin up and spin down DOS and their shifting below T_c. The sharp drop in S across the martensitic transition suggests that there is an enhancement of DOS at E_F. However, the drop in the κ across this transi-

tion cannot be accounted by similar arguments. We interpreted this as due to the scattering of conduction electrons and phonons by the disorder introduced into the system during the martensitic transition. In presence of magnetic field, the martensitic transition shifts to lower temperatures leading to large values of magnetothermoelectric power and magnetothermal conductivity in the vicinity of martensitic transition. An interesting feature of thermal transport properties is the absence of a peak in their temperature dependence below 50 K. This arises from the suppression of umklapp phonon-phonon, and phonon-electron process due to scattering from impurities and boundaries.

ACKNOWLEDGMENTS

L.S.S.C. would like to thank BRNS, DAE, India for the financial assistance (KSKRA).

[1] Y. Sutou, Y. Imano, N. Koeda, T. Omori, R. Kainuma, K. Ishida, and K. Oikawa, Appl. Phys. Lett. **85**, 4358 (2004).
[2] S. Y. Yu, Z. H. Liu, G. D. Liu, J. L. Chen, Z. X. Cao, G. H. Wu, B. Zhang, and X. X. Zhang, Appl. Phys. Lett. **89**, 162503 (2006).
[3] V. K. Sharma, M. K. Chattopadhyay, K. H. B. Shaeb, Anil Chouhan, and S. B. Roy, Appl. Phys. Lett. **89**, 222509 (2006).
[4] T. Krenke, M. Acet, E. F. Wassermann, X. Moya, L. Manosa, and A. Planes, Phys. Rev. B **73**, 174413 (2006).
[5] V. K. Sharma, M. K. Chattopadhyay, and S. B. Roy, J. Phys. D **40**, 1869 (2007).
[6] V. K. Sharma, M. K. Chattopadhyay, Ravi Kumar, Tapas Ganguli, Pragya Tiwari, and S. B. Roy, J. Phys.: Condens. Matter **19**, 496207 (2007).
[7] X. Moya, L. Manosa, A. Planes, S. Aksoy, M. Acet, E. F. Wassermann, and T. Krenke, Phys. Rev. B **75**, 184412 (2007).
[8] V. K. Sharma, M. K. Chattopadhyay, and S. B. Roy, J. Phys.: Condens. Matter **20**, 425210 (2008).
[9] V. K. Sharma, M. K. Chattopadhyay, and S. B. Roy, Phys. Rev. B **76**, 140401(R) (2007).
[10] M. K. Chattopadhyay, V. K. Sharma, and S. B. Roy, Appl. Phys. Lett. **92**, 022503 (2008).
[11] V. K. Sharma, M. K. Chattopadhyay, A. Chouhan, and S. B. Roy, J. Phys. D **42**, 185005 (2009).
[12] A. Planes, L. Manosa, and M. Acet, J. Phys.: Condens. Matter **21**, 233201 (2009) and the references therein.
[13] B. Zhang, X. X. Zhang, S. Y. Yu, J. L. Chen, Z. X. Cao, and G. H. Wu, Appl. Phys. Lett. **91**, 012510 (2007).
[14] K. R. Priolkar, P. A. Bhobe, S. D. Sapeco, and R. Paudel, Phys. Rev. B **70**, 132408 (2004).
[15] Y. K. Kuo, K. M. Sivakumar, H. C. Chen, J. H. Su, and C. S. Lue, Phys. Rev. B **72**, 054116 (2005).
[16] P. A. Bhobe, J. H. Monteiro, J. C. Cascalheira, S. K. Mendiratta, K. R. Priolkar, and P. R. Sarode, J. Phys.: Condens. Matter **18**, 10843 (2006).
[17] G. Li, Y. Liu, and B. K. A. Ngoi, J. Magn. Magn. Mater. **303**, 261 (2006).
[18] K. Koyama, T. Igarashi, H. Okada, K. Watanabe, T. Konomata, R. Kainuma, W. Ito, K. Oikawa, and K. Ishida, J. Magn. Magn. Mater. **310**, e994 (2007).
[19] See, e.g., R. D. Barnard, *Thermoelectricity in Metals and Alloys* (Taylor & Francis, London, 1972).
[20] See, e.g., F. J. Blatt, P. A. Schroeder, C. L. Foiles, and D. Greig, *Thermoelectric Power of Metals* (Plenum Press, New York, 1976).
[21] S. C. Jain, V. Narayan, and T. C. Goel, J. Phys. D **2**, 101 (1969).
[22] Technical notes/Measurement Manual, Quantum Design (2005).
[23] O. Maldonado, Cryogenics **32**, 908 (1992).
[24] http://elk.sourceforge.net
[25] J. P. Perdew, A. Ruzsinszky, G. I. Csonka, O. A. Vydrov, G. E. Scuseria, L. A. Constantin, X. Zhou, and K. Burke, Phys. Rev. Lett. **100**, 136406 (2008).
[26] See, e.g., P. M. Chaikin and T. C. Lubensky, *Principles of Condensed Matter Physics* (Chambridge University Press, Chambridge, 2000).
[27] See, e.g., J. Yang, in *Thermal Conductivity: Theory, Properties and Applications (Physics of Solids and Liquids)*, edited by T. M. Tritt (Springer, Berlin, 2005).
[28] Y. Noda and Y. Ishikawa, J. Phys. Soc. Jpn. **40**, 690 (1976).
[29] S. P. McAlister, I. Shiozaki, C. M. Hurd, and C. V. Stager, J. Phys. F: Met. Phys. **11**, 2129 (1981).
[30] Y. V. Kudryavtsev, Y. P. Lee, and J. Y. Rhee, Phys. Rev. B **69**, 195104 (2004).
[31] C. Biswas, R. Rawat, and S. R. Barman, Appl. Phys. Lett. **86**, 202508 (2005).
[32] J. Kübler, A. R. William, and C. B. Sommers, Phys. Rev. B **28**, 1745 (1983).
[33] A. Hamzic, R. Asomoza, and I. A. Campbell, J. Phys. F: Met. Phys. **11**, 1441 (1981).
[34] J. Y. Lee, G. C. McIntosh, A. B. Kaiser, Y. W. Park, M. Kaack, J. Pelzl, C. K. Kim, and K. Nahm, J. Appl. Phys. **89**, 6223 (2001).
[35] C. S. Garde, J. Ray, and G. Chandra, J. Phys.: Condens. Matter **1**, 2737 (1989).
[36] J. B. Sousa, M. E. Braga, F. C. Correia, F. Carpinteiro, L. Morellon, P. A. Algarabel, and R. Ibarra, J. Appl. Phys. **91**, 4457 (2002).
[37] R. P. Pinto, J. B. Sousa, F. C. Correia, J. P. Araujo, M. E. Braga, A. M. Pereira, L. Morellon, P. A. Algarabel, C. Magen, and R. Ibarra, J. Magn. Magn. Mater. **290-291**, 661 (2005).
[38] A. M. Pereira, C. Magen, J. P. Araujo, P. A. Algarabel, L. Morellon, M. E. Braga, R. P. Pinto, R. Ibarra, and J. B. Sousa, J. Magn. Magn. Mater. **310**, e580 (2007).
[39] L. S. Sharath Chandra, A. Lakhani, D. Jain, S. Pandya, P. N. Vishwakarma, M. Gangrade, and V. Ganesan, Rev. Sci. Instrum. **79**, 103907 (2008).
[40] C. S. Lue, Y.-K. Kuo, S.-N. Hong, S. Y. Peng, and C. Cheng, Phys. Rev. B **71**, 064202 (2005).
[41] G. Bihlmayer, R. Eibler, and A. Neckel, J. Phys.: Condens. Matter **5**, 5083 (1993).
[42] S. R. Barman, S. Banik, and Aparna Chakrabarti, Phys. Rev. B

72, 184410 (2005).
[43] S. R. Barman, and Aparna Chakrabarti, Phys. Rev. B **77**, 176401 (2008).
[44] See, e.g. G. Grimvall, *Thermophysical Properties of Materials* (North-Holland, Amsterdam, 1999).
[45] T. Aisaka and M. Shimizu, J. Phys. Soc. Jpn. **28**, 646 (1970).
[46] A. G. A. M. Saleh and N. H. Saunders, J. Magn. Magn. Mater. **29**, 197 (1982).